DCLRE1B/Apollo germline mutations associated with renal cell carcinoma impair telomere protection

Charlie Bories, Thomas Lejour, Florine Adolphe, Laëtitia Kermasson, Sophie Couvé, Laura Tanguy, Gabriela Luszczewska, Manon Watzky, Victoria Poillerat, Pauline Garnier, et al.

BBA - Molecular Basis of Disease 1870 (2024) 167107

Contents lists available at ScienceDirect

BBA - Molecular Basis of Disease

journal homepage: www.elsevier.com/locate/bbadis

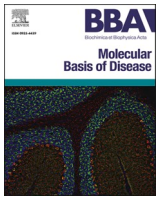

DCLRE1B/Apollo germline mutations associated with renal cell carcinoma impair telomere protection

Charlie Bories [a,b], Thomas Lejour [a,b], Florine Adolphe [a,b], Laëtitia Kermasson [c], Sophie Couvé [a,b], Laura Tanguy [a,b], Gabriela Luszczewska [a,b], Manon Watzky [a,b], Victoria Poillerat [a,b], Pauline Garnier [a,b], Regina Groisman [b], Sophie Ferlicot [b,d], Stéphane Richard [a,b,e], Murat Saparbaev [b], Patrick Revy [c], Sophie Gad [a,b], Flore Renaud [a,b,*]

[a] EPHE, PSL Université, Paris, France
[b] UMR 9019 CNRS, Gustave Roussy, Université Paris-Saclay, 114 rue Edouard Vaillant, Villejuif 94800, France
[c] Laboratory of Genome Dynamics in the Immune System, Laboratoire labellisé Ligue Nationale contre le Cancer, INSERM UMR 1163, Université de Paris, Imagine Institute, Paris, France
[d] Département de Pathologie, AP-HP, Université Paris-Saclay, Hôpital de Bicêtre, Le Kremlin-Bicêtre, France
[e] Réseau National de Référence pour Cancers Rares de l'Adulte PREDIR labellisé par l'INCa, Hôpital de Bicêtre, AP-HP, et Service d'Urologie, Le Kremlin-Bicêtre, France

ARTICLE INFO

Keywords:
DCLRE1B/Apollo
Renal cell carcinoma
Germline mutations
Telomere
DNA repair

ABSTRACT

Hereditary renal cell carcinoma (RCC) is caused by germline mutations in a subset of genes, including *VHL*, *MET*, *FLCN*, and *FH*. However, many familial RCC cases do not harbor mutations in the known predisposition genes. Using Whole Exome Sequencing, we identified two germline missense variants in the *DCLRE1B/Apollo* gene (*Apollo*^{N246I} and *Apollo*^{Y273H}) in two unrelated families with several RCC cases. *Apollo* encodes an exonuclease involved in DNA Damage Response and Repair (DDRR) and telomere integrity. We characterized these two functions in the human renal epithelial cell line HKC8. The decrease or inhibition of *Apollo* expression sensitizes these cells to DNA interstrand crosslink damage (ICLs). HKC8 *Apollo*$^{-/-}$ cells appear defective in the DDRR and present an accumulation of telomere damage. Wild-type and mutated Apollo forms could interact with TRF2, a shelterin protein involved in telomere protection. However, only Apollo^{WT} can rescue the telomere damage in HKC8 *Apollo*$^{-/-}$ cells. Our results strongly suggest that Apollo^{N246I} and Apollo^{Y273H} are loss-of-function mutants that cause impaired telomere integrity and could lead to genomic instability. Altogether, our results suggest that mutations in *Apollo* could induce renal oncogenesis.

1. Introduction

Renal Cell Carcinoma (RCC) account for ~300,000 new cases and ~100,000 deaths yearly worldwide [1]. RCC arise from the renal tubular epithelium and include multiple subtypes based on their histology and genetics [1,2], with clear cell RCC (ccRCC, 75 %), papillary RCC (pRCC, 15 %) and chromophobe RCC (chRCC, 5 %) being the major subtypes. Inherited diseases have been associated with an increased risk of RCC development, including von Hippel-Lindau (VHL), Hereditary Papillary Renal Carcinoma (HPRC), Birt–Hogg–Dubé (BHD) and Hereditary Leiomyomatosis and RCC (HLRCC)-associated RCC. Inherited RCC account for 3–5 % of all RCC cases and remain minor compared to sporadic cases. However, investigating the mechanisms driving cancer development in inherited RCC led to significant advances in understanding renal oncogenesis in both inherited and sporadic RCC [1,3]. Indeed, the *VHL* tumor suppressor gene, that notably regulates the hypoxia-inducible transcription factors (HIF), was first identified in VHL patients and subsequently found to be altered at somatic level in the majority of sporadic ccRCC [4,5]. The identification of *VHL* mutations driving ccRCC tumors was a breakthrough in the sporadic ccRCC therapeutic landscape, leading to the emergence of treatments targeting the VHL/HIF signaling pathway in ccRCC patients [6]. Other major sporadic RCC-associated genes [5,7,8] including *MET*, *PTEN*, *BAP1*, and *PBRM1* were similarly identified as germline events in familial RCC [9–12]. While the predisposing genes remain to be identified in many hereditary RCC cases, the existence of recurrent parallels between sporadic and familial RCC further emphasizes the necessity to search for additional driver genes in such familial cases.

* Corresponding author at: EPHE, PSL Université, Paris, France ; UMR 9019 CNRS, GR, U. Paris-Saclay, Villejuif, France.
E-mail address: flore.renaud-paitra@gustaveroussy.fr (F. Renaud).

https://doi.org/10.1016/j.bbadis.2024.167107
Received 5 July 2023; Received in revised form 14 February 2024; Accepted 25 February 2024
Available online 29 February 2024

ccRCC is characterized by high genomic instability, including large somatic copy number alterations (SCNA) [5,13]. Although defective DNA Damage Response and Repair (DDRR) pathways are classically associated with genomic instability, genetic alterations in genes related to DDRR pathways are not usually associated with RCC. However, recent studies provided evidence pointing towards a paradigm shift. In particular, the DDRR-targeted sequencing study by Hartman and colleagues revealed the existence of germline pathogenic variants in DDRR genes in 8.55 % of patients with early-onset RCC [14]. DDRR-associated gene variants were also reported in 25 % (somatic) and 19 % (somatic and germinal) of patients with locally advanced ccRCC and metastatic ccRCC, respectively [15,16]. Another study reported alterations in the expression of DDRR-associated genes in ccRCC, and identified six DDRR gene-signatures associated with ccRCC patient prognosis [17]. Finally, defective DDRR pathways in RCC tissues or cell lines could be associated with *VHL* or *PBRM1* defects and an increase in PARP inhibitors sensitivity [18–20]. The study of DDRR-associated genes in renal oncogenesis should be pursued to improve RCC patient prognosis and develop new therapeutic strategies targeting DDRR pathways.

The *DCLRE1B* gene (DNA Cross-Link Repair 1B) encodes the SNM1B protein, also known as Apollo (name used hereafter for gene and protein). This gene, located at 1p13.2, is composed of 4 exons encoding a 532 amino-acid protein. Apollo is a 5′ → 3′ exonuclease involved in two fundamental processes related to genome stability: DNA repair and telomere integrity [21]. Indeed, Apollo is involved in the repair of DNA interstrand crosslinks (ICLs) [22–25], stalled replication forks [26], and double-strand breaks (DSBs) [23,24]. In addition, Apollo localizes at and protects telomeres *via* its interaction with TRF2 [24,27–30], a member of the shelterin complex (including TRF1, TRF2, TIN2, RAP1, TPP1, and POT1) in charge of telomere maintenance and integrity [31]. *Apollo* downregulation or deletion leads to the accumulation of dysfunctional telomeres [27,30,32–34]. Studies in *Apollo*$^{-/-}$ mouse embryonic fibroblasts (MEFs) revealed that Apollo is involved in the generation, at the leading-end telomeres, of the 3′ terminal single-stranded structure, called G-overhang, essential for proper binding of the shelterin complex and formation of the T-loop [32,33,35]. In mice, *Apollo* knockout induces perinatal lethality [36]. In humans, an *Apollo* splice variant and germline biallelic mutations were characterized in patients presenting Hoyeraal-Hreidarsson syndrome (HH), one of the most severe forms of telomere biology disorders [34,37,38]. In addition, *Apollo* single nucleotide polymorphisms (SNPs) were associated with breast cancer and melanoma [39–41] while one chromosomal breakpoint region located within intron 3 of *Apollo* was associated with Wilms tumor, a pediatric kidney cancer [42].

In this study, we identified two heterozygous germline missense variants in the *Apollo* gene in two families with inherited ccRCC and no germline mutations in the common RCC-associated genes. We investigated the functional impact on the genome integrity of these variants in renal cells. In the HKC8 human renal cell model, we observed an important role for *Apollo* in the response to DNA ICLs and the protection of telomeres. Notably, we demonstrated a failure of the *Apollo* mutants to preserve telomere integrity, suggesting they could cause genomic instability and favor tumorigenesis.

2. Materials and methods

2.1. Patient samples

The two families gave written informed consent for research and blood samples. Family A includes 2 sibling patients, affected only by ccRCC at 34 and 55 years old respectively (Fig. 1A). Family B comprises 3 patients affected only by ccRCC at 44, 47, and 62 years old respectively, and one affected only by cutaneous melanoma at 60 years old. Bone metastasis was recently detected in patient B-III.1. As ccRCC segregated at young ages in both families, they were referred for genetic testing. Known RCC predisposition genes were sequenced and no germline mutation was detected. One ccRCC fixed tumor was available from each family, which was reviewed by a referent senior uropathologist (SF) who confirmed the diagnosis. Lymphoblastoid cell lines (LLB) were established. DNA was extracted from blood and tumor samples, as previously described [43].

2.2. Genetic analyses

Whole Exome Sequencing (WES) was performed on blood samples for families A and B as previously described [43]. Raw data can be obtained using European Genome-phenome Archive number EGAS50000000216.

Sanger sequencing was used i) to confirm variants in *DCLRE1B/Apollo* and for tumor analysis, and ii) to verify the sequence of *Apollo* transcripts in LLB. The reference sequence used for annotations is NM_022836.4. For *in silico* analyses, we used different tools included in the free software MobiDetails (Inserm, France).

2.3. Apollo expression vectors

The wild-type human *DCLRE1B/Apollo* coding sequence cloned in pBlueScript II Vector (pBSII) was purchased from GeneCust (France). The *Apollo* mutations c.737A>T, p.N246I and c.817T>C, p.Y273H were generated using the QuickChange II XL Site-Directed Mutagenesis Kit (Agilent Technologies, Santa Clara, CA, USA) according to the manufacturer's protocol. Then, wild-type and mutated *Apollo* sequences were subcloned into pcDNATM3.1/myc-His vector (Invitrogen, Life Technologies, CA, USA) to express the C-terminal myc-His tagged wild-type or mutant Apollo (named Apollo^{WT}, Apollo^{N246I}, Apollo^{Y273H}).

2.4. Cell culture and transfection

The Human Kidney Cell Clone 8 (HKC8) is an SV40-Ad12 immortalized cell line from kidney epithelial cells (a kind gift from LC Racusen [44]). Cells were cultured in Dulbecco's Modified Eagle Medium (DMEM) supplemented with 10 % Foetal Bovine Serum (FBS) and 100 μg/mL penicillin-streptomycin (PS) at 37 °C and 5 % CO2. LLB were cultivated in Roswell Park Memorial Institute medium (RPMI) supplemented with 10 % FBS and 100 μg/mL PS.

Cells were transfected using FuGENE® HD Transfection Reagent (Promega, WI, USA) at a 3:1 ratio FuGENE®:DNA (μL:μg) according to the manufacturer's protocol.

For transient transfections, cells were collected 48 h post-transfection. For stable transfections, 1 mg/mL of geneticin was added to the culture medium 48 h post-transfection. Cells were then cultured for 2 weeks under constant selection pressure before processing.

2.5. CRISPR Cas9 knockout

Guide RNA sequence was cloned into the pSpCas9(BB)-2A-GFP (PX458), a gift from Feng Zhang (Addgene plasmid # 48138, MA, USA). The genomic sequence targeted for CRISPR-Cas9 disruption in the *DCLRE1B/Apollo* gene was 5′-GTCCACTGCGATGGGCGTAT-3′. HKC8 cells were transfected using Lipojet™ transfection reagent (SignaGen Laboratories # SL100468, MD, USA) following the manufacturer's instructions. GFP+ cells were selected 48 h post-transfection using a BD FACSAria™ III cell sorter (BD Biosciences, NJ, USA). Single clones were extended and putative *Apollo* knockout cells were identified using RT-qPCR.

2.6. siRNA-mediated downregulation

Apollo mRNA was targeted using the ON-TARGETplus Human DCLRE1B siRNA - SMART pool (Dharmacon, L-015780-00-0005, CO, USA). The ON-TARGETplus Non-targeting Control Pool (Dharmacon, D-

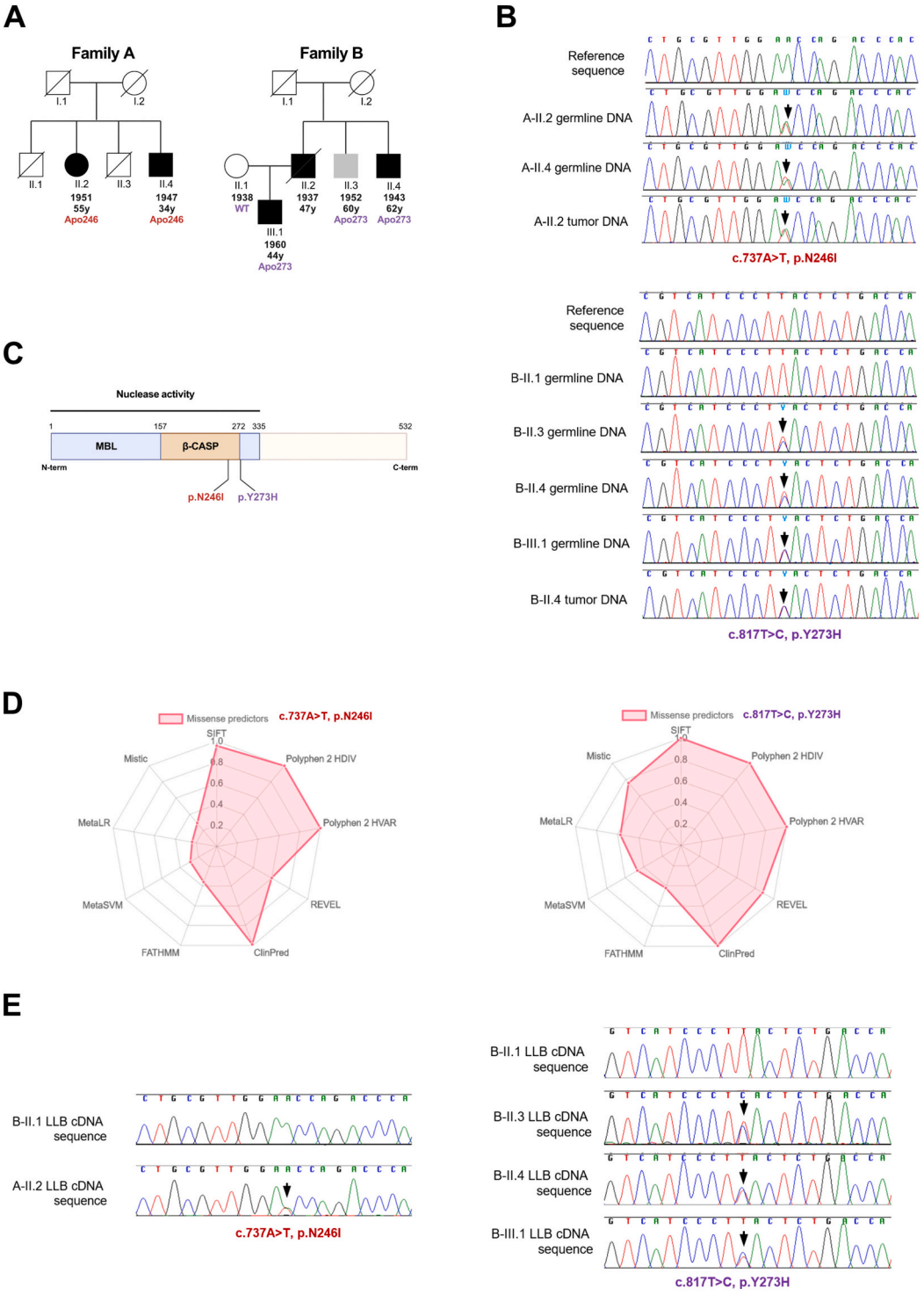

Fig. 1. Identification of missense variants in the *Apollo* gene within two different families affected by ccRCC. A Pedigree of the two families. Patients affected with ccRCC are in black (except one in gray with melanoma). Birth date and age of diagnosis are indicated below symbols, with *Apollo* status after sequencing of blood DNA: wild-type (WT) or mutated with the specific mutation (corresponding to amino-acid 246 for family A and 273 for family B). **B** Sequencing of the *Apollo* gene for individuals from pedigrees showed in A. The chromatograms correspond to Sanger sequencing of families A (higher panel) and B (lower panel). The arrows show the corresponding missense variants detected in either germline or tumor DNA extracted from available patient samples. **C** Schematic representation of the Apollo protein. The 532 amino-acid isoform contains two domains that exert the nuclease activity: metallo-β-lactamase (MBL) and β-CPSF-Artemis-SNM1-PSO2 (β-CASP). Both missense variants identified in families presented in A are indicated by the same color code. **D** Partial results extracted from MobiDetails software report for *in silico* analyses of missense variants detected in *Apollo* in families A (left panel) and B (right panel). These polar graphs present 9 tools used to estimate the functional impact of the amino acid changes of the protein; the larger the pink zone, the more deleterious effect on the function. Both variants identified in *Apollo* are evaluated as probably damaging. **E** Sequencing chromatograms showing the *Apollo* sequence of cDNA obtained from lymphoblastoid cell line (LLB) transcripts for both families.

001810-10-05) was used as control. Cells seeded in 6-well plates were transfected with 110 pmols siRNA using the Lipofectamine® RNAiMAX Reagent (ThermoFisher Scientific, MA, USA) according to the manufacturer's protocol.

2.7. Reverse transcription and quantitative PCR (RT-qPCR)

Total RNA was extracted from cell pellets using the NucleoSpin RNA Kit (Macherey Nagel, Germany) according to the manufacturer's protocol. mRNA reverse transcription was performed on 1 μg of total RNA using the High Capacity cDNA Reverse Transcription Kit (ThermoFisher Scientific) plus RNaseOUT Ribonuclease Inhibitor (ThermoFisher Scientific). cDNA was amplified in the Master Mix Select SYBR® (ThermoFisher Scientific) with the CFX96 Touch Real-Time PCR Detection System (BioRad, CA, USA). *Peptidylpropyl isomerase* (*PPIA*) and *hypoxanthine phosphoribosyl* (*HPRT1*) were used as control genes. Analysis was performed using the CFX Maestro software (BioRad). The sequences of the primers used are: Apollo_Primer_1_For: 5′-CACCTC TTGCATCGTCACCT-3′; Apollo_Primer_1_Rev: 5′-GGAGGGTTACGGT-CATGGTC-3′; Apollo_Primer_2_For: 5′-CCTGGTTCTTCCTTCCCGACAA-3′; Apollo_Primer_2_Rev: 5′-TCCTTTCCCAGGCTGTAGAGTC-3′; PPIA_-For: 5′-GCCGAGGAAAACCGTGTACT-3′; PPIA_Rev: 5′-CTGCAAACAGCT CAAAGGAGAC-3′; HPRT1_For: 5′-TTGCTTTCCTTGGTCAGGCA-3′; HPR T1_Rev: 5′-ATCCAACACTTCGTGGGGTC-3′.

2.8. Survival assay

Cells were seeded at 5000 cells/well in 24-well plates and left to attach for 3-4 h before adding increasing doses of genotoxic drugs to the culture medium. Survival was related to cell confluence monitored by the Incucyte® S3 Live-Cell Analysis System (Sartorius, Germany) 6 days after treatment.

2.9. Immunoprecipitation, Western blotting, and mass spectrometry

Cells were lysed for 15 min on ice in Pierce™ IP Lysis Buffer (ThermoFisher Scientific) supplemented with Halt™ Protease and Phosphatase Inhibitor Cocktail (ThermoFisher Scientific). One mg of lysate was incubated with 50 μL Anti-c-Myc beads (A7470, Sigma Aldrich, MO, USA) for 2 h at 4 °C under agitation. Elution was performed by incubating beads with 150 ng/μL c-Myc Peptide (M2435, Sigma-Aldrich) for 1 h at 4 °C under agitation. Immunoprecipitated and input fractions were analyzed by Western blotting with anti-DCLRE1B (A6808, ABclonal, MA, USA) and anti-TRF2 (NB110-57130, Novus Biologicals, Bio-techne, MN, USA) and HRP-coupled anti-rabbit antibody (4010-05, Southern Biotech, AL, USA).

For mass spectrometry analysis, proteins were concentrated using trichloroacetic acid (TCA) precipitation. Briefly, immunoprecipitated proteins were resuspended in 20 % TCA and incubated for 15 min on ice before centrifugation at 13,000*g* for 20 min at 4 °C. Pellets were resuspended in 10 % TCA and washed twice in cold acetone with intermediate centrifugations at 13,000*g* for 10 min at 4 °C. Finally, samples were air-dried and sent for analysis to the Taplin Biological Mass Spectrometry Facility (Harvard Medical School, Boston, USA).

2.10. Immunofluorescence

Cells grown in 12 Well Chamber slides (Ibidi®, Germany) were fixed with 2 % paraformaldehyde for 10 min, permeabilized with 0.1 % Triton X-100 for 30 min and incubated with anti-53BP1 (4937, CST, MA, USA) or anti-γH2AX (05-636, Merck) for 1 h at RT. After washing with PBS, cells were incubated with anti-rabbit Alexa Fluor® 488 Conjugate (4412, CST) or anti-mouse Alexa Fluor® 594 Conjugate (8890, CST) for 30 min at RT. Slides were next stained with VECTASHIELD® with DAPI (Vector Laboratories, CA, USA). Analysis was performed with ImageJ.

2.11. Chromosome FISH

Cells were arrested in metaphase with 100 ng/mL Colcemid™ KaryoMAX™ (ThermoFisher Scientific) for 1 h before collection and resuspension in hypertonic 75 mM KCl solution for 20 min at 37 °C. Cells were then fixed in 3:1 methanol/acetic acid (vol:vol) and dropped onto glass slides. Metaphases were fixed in 4 % formaldehyde for 2 min and dehydrated with successive 2 min incubations in 70 %, 90 %, and 100 % ethanol. The telomeric TelC-Cy3 probe (PNA Bio Inc., CA, USA) was spread on slides after dilution at 500 nM in 70 % formamide, 20 mM Tris-HCl pH 7.4, and 1 % Blocking Reagent (Roche, Switzerland). DNA was denatured at 80 °C for 5 min and hybridized at RT for 1 h30 in the dark. Slides were washed 2 × 15 min in 70 % formamide and 3 × 5 min in 50 mM Tris-HCl pH 7.4, 150 mM NaCl, and 0.05 % Tween-20. Slides were next dehydrated with successive 70 %, 90 %, and 100 % ethanol baths and stained with VECTASHIELD® with DAPI (Vector Laboratories). Analysis was performed with ImageJ.

3. Results

3.1. Identification of two missense variants in DCLRE1B/Apollo gene in two families with clear cell RCC

The two families studied presented two (family A) and three (family B) affected cases of clear cell RCC (ccRCC) (Fig. 1A). As no germline mutation was detected in known RCC predisposition genes, we searched by Whole Exome Sequencing (WES) for the presence of potentially pathogenic variants in new genes. The common point between the two families was the presence of a germline missense variant detected in the *DCLRE1B/Apollo* gene co-segregating with ccRCC (Fig. 1B). Affected individuals from family A carried a c.737A>T, p.Asn246Ile (*i.e.* N246I) *Apollo* variant while affected individuals from family B harbored a c.817T>C, p.Tyr273His (*i.e.* Y273H) *Apollo* variant. In both families, the variants were identified at heterozygous state. The *Apollo* variants were also detected in the available tumors with a heterozygous profile consistent with no loss of heterozygosity (LOH). Both variants are not reported in databases including large sequencing studies on normal populations (gnomAD), patient cohorts (Clinvar) and tumor series (COSMIC). Both *Apollo* missense variants are located in the metallo-β-lactamase (MBL) domain or the β-CPSF-Artemis-SNM1-PSO2 (β-CASP) domain that are involved in its exonuclease activity [45] (Fig. 1C). To evaluate the possible impact of these variants, an *in silico* analysis was performed using MobiDetails. The different tools included in this package analyze the conservation of the protein sequence across species, the physico-chemical characteristics of the exchanged amino acids and estimate a putative deleterious effect. These tools predicted a high impact and a damaging effect of both *Apollo* variants (Fig. 1D). Finally, we tested whether the variants could affect the *Apollo* transcripts' stability. Sanger sequencing of *Apollo* cDNA obtained from the affected patient's lymphoblastoid cell lines (LLB) similarly detected the wild-type and mutated sequences (Fig. 1E). This result indicates that the two variants do not affect the stability of *Apollo* mRNA.

3.2. Effect of Apollo downregulation and deletion on DNA repair in human renal epithelial cells

Apollo was reported to be involved in the DNA repair of ICLs and DSBs [22–25]. However, its DNA repair activity was never studied in human renal epithelial cells. To this end, we decided to study Apollo's activities in the HKC8 (Human Kidney Clone 8) cell line derived from a healthy human renal proximal tubular epithelium [44]. Indeed, similarly to ccRCC tumors, HKC8 cells originate from the human renal epithelium. Moreover, HKC8 are non-tumoral cells, supporting their use in the context of a study focusing on the primary steps of renal oncogenesis. Thus, we investigated the impact of *Apollo* downregulation in the HKC8 cell line on *Apollo* mRNA levels and cell fate (proliferation,

survival, and cell death), both in the absence or presence of genotoxic drugs. HKC8 cells were transfected with a siRNA pool targeting *Apollo* (siApo) for 24 h before adding ICL-inducing (cisplatin) or DSB-inducing (etoposide) drugs for an additional 16–24 h. In HKC8 cells, the amount of endogenous Apollo is too low to be detected by Western blotting, even after immunoprecipitation, as previously reported in other cell models [23,27,30,46]. We then assessed the knockdown efficiency by RT-qPCR and demonstrated that *Apollo* mRNA level was decreased by >80 % compared to cells transfected with a siRNA control (siCtrl), both with and without genotoxic treatment (Fig. 2A). In siCtrl HKC8 cells, a significant increase in the *Apollo* mRNA level was detected upon cisplatin treatment compared to untreated cells, suggesting an upregulation and/or mRNA stabilization in response to this ICL-inducing drug. On the other hand, the *Apollo* mRNA level was not modified upon treatment with etoposide in these cells.

To determine the impact of *Apollo* downregulation in response to ICLs and DSBs, we evaluated the long-term survival of HKC8 cells in the presence of increasing drug concentrations over 6 days. *Apollo*

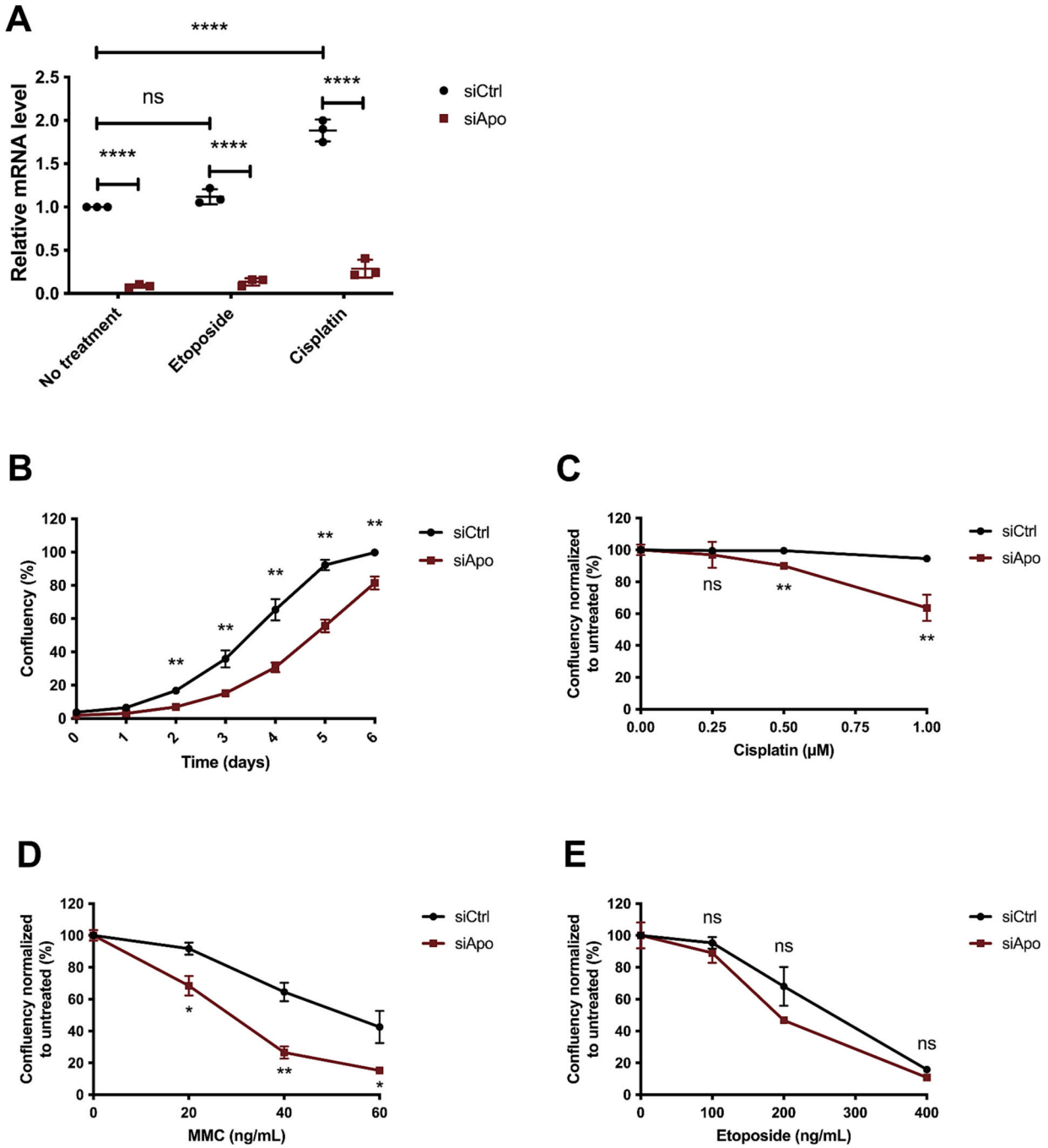

Fig. 2. Effect of *Apollo* downregulation on proliferation and survival in human renal epithelial cells. A *Apollo* transcripts quantification relative to control genes *PPIA* and *HPRT1* in the HKC8 cells transfected with siRNA targeting *Apollo* (siApo) or non-specific siRNA (siCtrl). Cells were treated with etoposide (25 µg/mL) or cisplatin (25 µM) for 16 h. Mean and standard deviation of 3 independent experiments. Statistics derived from two-way ANOVA with $\alpha = 0.05$. ns: non-significant, **: $p < 0.01$, ***: $p < 0.001$, ****: $p < 0.0001$. **B** Proliferation of siApo and siCtrl HKC8 cells without treatment over 6 days. Mean and standard deviation of biological triplicates are presented. Representative of 2 independent experiments. **C–E** Sensitivity of siApo and siCtrl HKC8 cells to increasing concentrations of cisplatin (C), mitomycin C (MMC) (D) and etoposide (E) after 6 days. Mean and standard deviation of biological triplicates. Representative of 2 independent experiments. Statistics derived from unpaired *t*-tests with $\alpha = 0.05$. ns: non-significant, *: $p < 0.05$, **: $p < 0.01$.

downregulation alone was sufficient to induce a reduced proliferation capacity of siApo HKC8 cells compared to control cells (Fig. 2B). Furthermore, *Apollo* knockdown increased the sensitivity of HKC8 cells to cisplatin and mitomycin C (MMC), another ICL-inducing drug (Fig. 2C). On the other hand, no difference was detected between siApo HKC8 and siCtrl HKC8 cells in the presence of etoposide (Fig. 2D). We also investigated the impact of *Apollo* downregulation on the cell cycle of HKC8 cells in response to the genotoxic drugs by flow cytometry. Compared to untreated cells, the percentage of siCtrl HKC8 was decreased in G1 and increased in G2/M upon etoposide treatment (Fig. S1A, B). On the other hand, the percentage of siCtrl HKC8 cells was decreased in G1 and increased in S upon cisplatin treatment. However, the percentage of cells in the different cell cycle phases was consistently similar between siCtrl HKC8 and siApo HKC8 cells in the absence and the presence of etoposide or cisplatin. In conclusion, the increased sensitivity of siApo HKC8 cells compared to siCtrl HKC8 cells in response to drug treatments is not due to differences in cell cycle regulation. Altogether, it suggests that the increased sensitivity of siApo HKC8 cells is probably due to a defective DDRR rather than cell cycle modification.

To further characterize the impact of Apollo deficiency in our renal cell line model, we generated CRISPR/Cas9-induced HKC8 knock-out (*Apollo*$^{-/-}$) cell lines. Among isolated clones, one showed the absence of *Apollo* mRNA when using two different pairs of primers (Fig. 3A, B). Consistent with the results obtained in siApo HKC8 cells, we observed a reduced proliferation of HKC8 *Apollo*$^{-/-}$ cells as compared to parental HKC8 cells while no difference in the cell cycle was observed between these two cell lines (Fig. 3C, Fig. S2A, B). The diminished proliferation capacity of HKC8 *Apollo*$^{-/-}$ was associated with an increased number of spontaneous 53BP1 and γH2AX foci, showing an accumulation of DNA damage (Fig. 3D, E). These results suggest that the endogenous cellular stress detected in HKC8 *Apollo*$^{-/-}$ cells may result from an impaired DNA repair pathway.

In accordance with the results obtained in siApo HKC8 cells, HKC8 *Apollo*$^{-/-}$ cells exhibited an increased sensitivity to cisplatin and MMC (Fig. 4A, B), while no difference was detected after etoposide treatment (Fig. 4C).

Overall, these results suggest that Apollo plays an important role in DNA repair in the absence of genotoxic stress or following ICLs induction in the human renal cell line HKC8, while it does not seem to participate in the repair of DSBs induced by etoposide in these cells.

3.3. Apollo-TRF2 interaction in HKC8 cells and study of the impact of the Apollo mutations

Apollo was reported to interact with many proteins in different cell models, including DNA repair proteins [21]. We then asked whether some of Apollo's partners could be detected in our renal cell model. To investigate these interactions, we carried out immunoprecipitation (IP) experiments against Myc in HKC8 cells transiently transfected with a Myc-tagged *Apollo* encoding vector or the corresponding empty vector. Fractions resulting from IP were analyzed by mass spectrometry. Apart from Apollo itself, the most abundant proteins identified in IP fractions were TRF2 and Rap1 (Fig. 5A).

While TRF2 is a well-known direct partner of Apollo, Rap1 interaction was previously suggested to be indirectly mediated through TRF2 [27]. As the interaction with TRF2 was reported to be essential for Apollo's location and activity at telomeres [30,32], we wondered whether the mutations could affect this interaction. Thus, we performed immunoblots (IB) following immunoprecipitations (IP) of cellular extracts from HKC8 cells transiently transfected with a vector encoding the different Myc-tagged forms of Apollo (Apollo^{WT}, Apollo^{N246I}, Apollo^{Y273H}). Similar levels of Apollo were detected in the input fractions indicating that the mutations did not affect protein stability, at least not in this exogenous context (Fig. 5B). In addition, no noticeable changes in TRF2 stability were detected upon expression of the different forms of Apollo. Finally, there was no significant impact of *Apollo* mutations on its interaction with TRF2 (Fig. 5B, C). As this interaction was unaffected by the mutations, it suggests that Apollo mutants keep the ability to localize at telomeres, raising the question of the functional impact of these mutations on telomere protection.

3.4. Apollo^{WT} protects telomeres in HKC8 cells by contrast to Apollo^{N246I} and Apollo^{Y273H} mutants

To explore the functional impact of Apollo mutants on telomere protection, we generated stable cell lines expressing the different forms of *Apollo* by transfecting HKC8 *Apollo*$^{-/-}$ cells with the Myc-tagged Apollo (Apollo^{WT}, Apollo^{N246I}, Apollo^{Y273H}) expression vectors. The transfected cells were kept under antibiotic selection pressure for two weeks to force integration of the *Apollo* transgenes into the genome. Despite this constant pressure, the *Apollo* mRNA levels in the resulting stable cell lines were only 25 % of those measured in parental HKC8 cells (Figs. 6A, 3A). This result was highly reproducible as similar mRNA levels were measured in four independent stable cell line transfection experiments. We hypothesized that high *Apollo* expression induced by the constitutive pCMV promoter may generate excessive cellular toxicity leading to the selection of low-expressing clones in our renal cell model. This toxicity would also explain why the endogenous Apollo protein level remains too low to be detected. Noteworthy, *Apollo* mRNA levels were similar between wild-type and mutants indicating that the mutations do not affect exogenous *Apollo* transcript stability, consistent with our previous results obtained for protein stability after transient transfections (Figs. 5B, 6A).

To assess telomere aberrations in our different cell lines, we performed chromosome Fluorescent *In Situ* Hybridization (FISH) with a DNA probe specifically targeting the telomere (TTAGGG)n repeats. This approach detected a significant increase in the frequency of telomere aberrations in the HKC8 *Apollo*$^{-/-}$ cell line transfected with the empty vector (Mock) as compared to the parental HKC8 cell line (Fig. 6B). This telomere phenotype was rescued upon *Apollo*^{WT} transfection, demonstrating a causal link between *Apollo* loss and telomere instability. Interestingly, transfection of either *Apollo*^{N246I} or *Apollo*^{Y273H} in HKC8 *Apollo*$^{-/-}$ cells did not reduce the rate of telomere aberrations, indicating a complete failure of the mutants to rescue the HKC8 *Apollo*$^{-/-}$ phenotype (Fig. 6B). The telomere aberrations detected in the *Apollo*^{N246I} and *Apollo*^{Y273H} expressing *Apollo*$^{-/-}$ HKC8 cell lines were similar to those of HKC8 *Apollo*$^{-/-}$ cells. This included an increase in the frequency of single and double telomeric signal losses (telomere loss and terminal deletion) (Fig. 6C, D) and a higher rate of telomere fusions as compared to HKC8 cells. An increase in sister chromatid fusions was also observed in *Apollo*$^{-/-}$ HKC8 cells expressing both mutants although only statistically significant in the *Apollo*$^{-/-}$ HKC8 cell line expressing *Apollo*^{Y273H}. In this setting, frequencies of dicentric chromosomes and multi-telomeric signals were rather low.

Overall, these results demonstrate that *Apollo* deletion in a human renal cell model results in an increased frequency of telomere aberrations reflecting defective telomere protection. Conversely to Apollo^{WT}, the mutants failed to rescue the telomere defects observed in the *Apollo*$^{-/-}$ HKC8 cell line. Thus, both *Apollo*^{N246I} and *Apollo*^{Y273H} are loss-of-function mutants regarding the telomere protective role of Apollo in human renal cells.

4. Discussion

Apollo is a key player in the maintenance of genome stability through its involvement in DNA repair and telomere protection. Associated with this last activity, *Apollo* was previously identified as a causal gene in the HH syndrome, a severe telomere biology disorder [34,37,38]. In our study, we identified two *Apollo* missense variants co-segregating with ccRCC in two unrelated families. These *Apollo* variants, also detected in tumor DNA, have never been reported elsewhere to the best of our knowledge. Analysis of the transcripts indicated that the

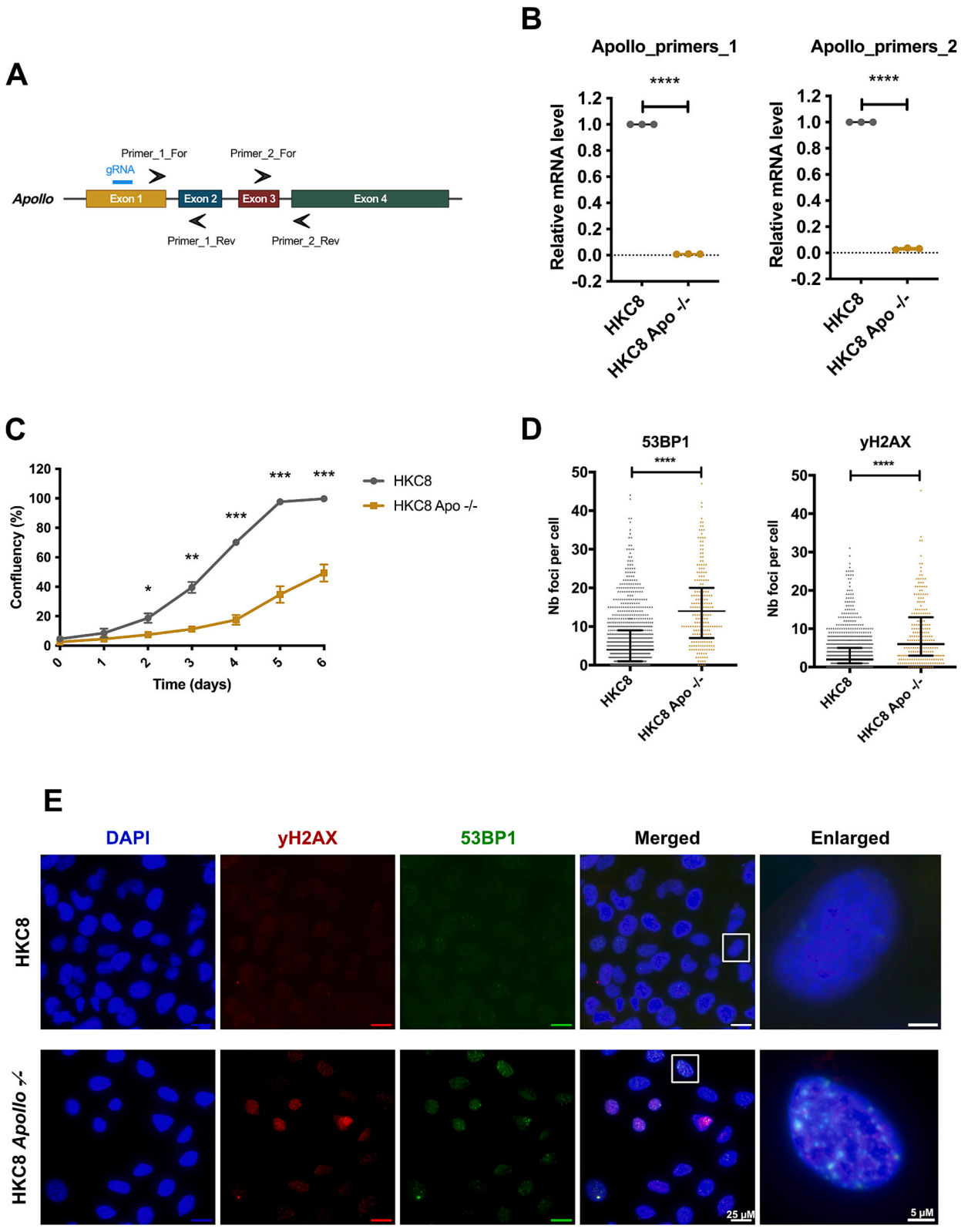

Fig. 3. Effect of *Apollo* knock-out on proliferation and DNA damage in human renal epithelial cells. A Schematic representation of the *Apollo* gene with the location of gRNA for CRISPR/Cas9 targeting and primer pairs 1 and 2 used in RT-qPCR. **B** *Apollo* transcripts quantification relative to control genes *PPIA* and *HPRT1* in parental and *Apollo*$^{-/-}$ HKC8 cells with both primer pairs by RT-qPCR. Mean and standard deviation of 3 independent experiments are represented. **C** Proliferation of parental and *Apollo*$^{-/-}$ HKC8 cells without treatment. Mean and standard deviation of biological triplicates are presented. Representative of 3 independent experiments. **D** Quantification of 53BP1 and γH2AX foci in untreated parental and *Apollo*$^{-/-}$ HKC8 cells. Median and interquartile range with n≥200. Representative of 3 independent experiments. **E** Representative pictures of 53BP1 and γH2AX foci in untreated parental and *Apollo*$^{-/-}$ HKC8 cells analyzed in D. All statistics are derived from unpaired *t*-tests with $\alpha = 0.05$. ns: non-significant, *: $p < 0.05$, **: $p < 0.01$, ***: $p < 0.001$, ****: $p < 0.0001$.

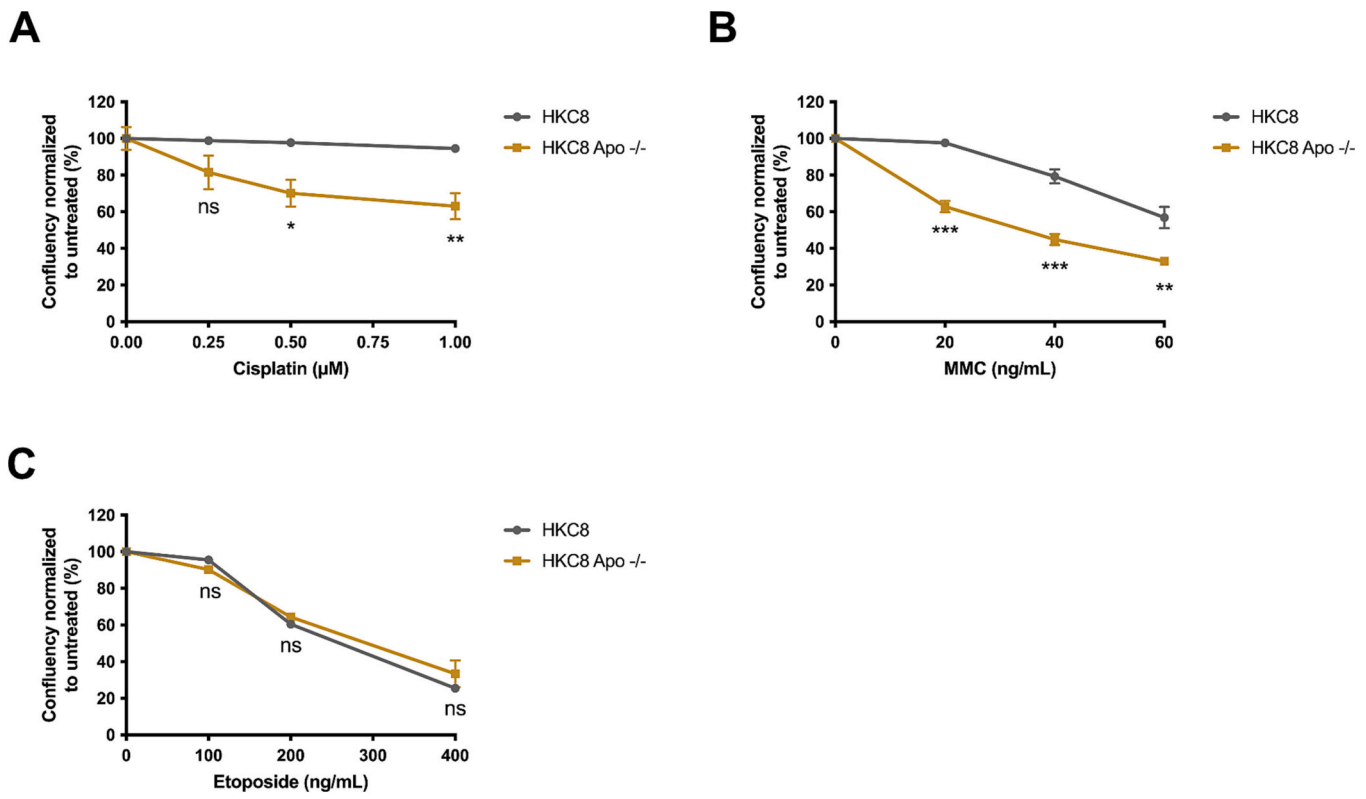

Fig. 4. Effect of *Apollo* knock-out on survival in human renal epithelial cells. A–C Sensitivity of parental and *Apollo*$^{-/-}$ HKC8 cells to increasing concentrations of cisplatin (A), mitomycin C (B) and etoposide (C) after 6 days. Mean and standard deviations of biological triplicates are represented. Representative of 3 independent experiments. All statistics are derived from unpaired *t*-tests with $\alpha = 0.05$. ns: non-significant, *: $p < 0.05$, **: $p < 0.01$, ***: $p < 0.001$.

variants do not impact *Apollo* mRNA stability and immunoblot similarly detected exogenous WT and mutated Apollo, indicating that the mutations do not impair Apollo protein stability. However, *in silico* analyses predicted the patients' mutations to be damaging, which prompted us to investigate the role of Apollo in human kidney cells and examine the functional impact of these mutants. This study was carried out in the non-cancerous HKC8 cell line originating from the human proximal renal tubular epithelium, a relevant model to study the possible role of Apollo in the initiation of renal oncogenesis.

Apollo was previously shown to be involved in the repair of ICLs, DSBs, and replicative stress in various cell lines but never in an epithelial renal cell model. The downregulation and deletion of *Apollo* in HKC8 cells resulted in an increased sensitivity to MMC and cisplatin, indicating a role for Apollo in the repair of ICLs, which was consistent with previously published data in other cell lines [22,23,25]. In contrast, no significant impact was detected in response to DSBs arising from exposure to etoposide, a topoisomerase 2 inhibitor. The involvement of Apollo in the repair of DSBs has been previously debated as Demuth and colleagues reported an impact of *Apollo* knockdown in response to ionizing radiation (IR)-induced DSBs in HeLa [23] and U2OS cells [46] while no effect was reported by other groups in HEK293T [22] and the DT40 chicken cell line [47]. Considering these different results, one can suggest that Apollo's role in response to DSBs may depend on multiple factors including species and cell types. Noteworthy, although ICLs and DSBs are often described as separated damage, the generation of DSBs is the step that follows ICL unhooking during the replication-coupled repair in the FANC/BRCA pathway. Since Apollo was shown to function in the FANC/BRCA pathway, it could be involved in DSBs processing in this context [25,46]. Interestingly, in the absence of exogenous stress, HKC8 *Apollo*$^{-/-}$ cells exhibited increased numbers of 53BP1 and γH2AX foci, indicating the generation of DNA damage. Apart from ICL repair, Apollo was also reported to participate in the FANC/BRCA pathway to solve replication stress caused by fork stalling [26]. Thus, the phenotype observed in the HKC8 *Apollo*$^{-/-}$ cell line may reflect the onset of DNA damage arising from such unresolved replicative stress.

Taken together, our results are consistent with a role for Apollo in the FANC/BRCA pathway for the resolution of endogenous and ICL-induced replicative stress in the renal cell line model HKC8. However, the precise role of Apollo in this pathway remains elusive and should be further investigated.

In agreement with other studies performed in different cell models, Apollo interacts with TRF2 in HKC8 cells. Recently, *Apollo* missense mutants affecting residue Leu142, even though outside of the TRF2-binding domain (amino acids 496 to 532), were shown to reduce the affinity for TRF2 [34], which prompted us to examine the impact of the *Apollo*^{N246I} and *Apollo*^{Y273H} mutations on this interaction. Our co-immunoprecipitation experiments did not reveal a significant impact of *Apollo*^{N246I} and *Apollo*^{Y273H} mutations regarding the Apollo-TRF2 interaction. This result supports the idea that Apollo^{N246I} and Apollo^{Y273H} could co-exist with Apollo^{WT} at telomeres in patients' cells. When studying telomere integrity in renal cells, we showed that the lack of *Apollo* resulted in a phenotype characterized by increased telomere damage, consistent with previous studies performed in other cells [27,30,32–34]. Telomere instability in the HKC8 *Apollo*$^{-/-}$ cells was rescued by the expression of *Apollo*^{WT}, but not by that of *Apollo*^{N246I} or *Apollo*^{Y273H}, suggesting that both of them are loss-of-function mutants regarding telomere protection. *Apollo*^{N246I} and *Apollo*^{Y273H} are respectively located in the β-CASP and MBL domains responsible for the nuclease activity of the protein. In particular, the *Apollo*^{Y273H} mutation is located in the essential “phosphate binding pocket” structure near the Asp275 residue which, when mutated, completely disrupts the nuclease activity [48]. Thus, the telomere phenotype reported in this study may be explained by the impairment or disruption of Apollo nuclease activity. This hypothesis is supported by the fact that the expression of Apollo nuclease-dead mutants fails to rescue telomere damage [32,33].

A

Gene symbol	Protein	Annotation	Nb Peptides (Unique)		
DCLRE1B	Apollo	5' exonuclease Apollo	13	9	19
TERF2	TRF2	Telomeric repeat-binding factor 2	12	8	5
TERF2IP	Rap1	Telomeric repeat-binding factor 2-interacting protein 1	10	9	7

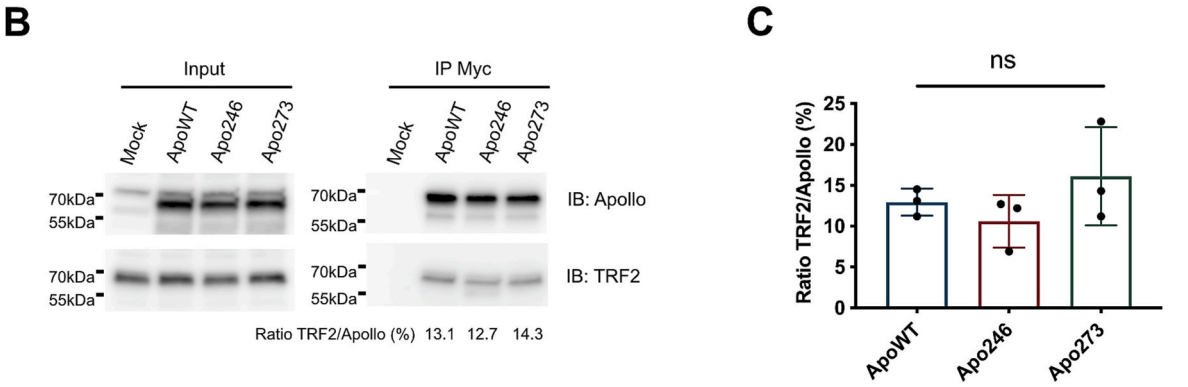

Fig. 5. WT and Apollo mutants similarly interact with TRF2 in the HKC8 cell line. A List of proteins identified by mass spectrometry that co-immunoprecipitated with Apollo WT-Myc. The number of unique peptides (peptide sequences assigned to a unique protein) is indicated for each of the 3 independent experiments performed. **B** Co-immunoprecipitation of endogenous TRF2 with exogenous Apollo^{WT}-Myc (ApoWT), Apollo^{N246I}-Myc (Apo246), or Apollo^{Y273H}-Myc (Apo273). Inputs represent 2 % of the total protein extracts used for immunoprecipitation. One mg of total protein extract was used for immunoprecipitation in all different conditions. Apollo and TRF2 signals were revealed at the same time and in the same conditions. Numbers under the gel indicate the band signal intensity of TRF2 relative to Apollo in the immunoprecipitated fractions. Mock: Empty vector. **C** Quantification of TRF2 relative to Apollo in the immunoprecipitated fractions as presented in B. Mean and standard deviations from 3 independent experiments are presented. Statistic derived from one-way ANOVA with $\alpha = 0.05$. ns: non-significant.

It would be interesting to study the nuclease activity of the Apollo mutants on DNA substrates *in vitro*. However, production of the full-length Apollo recombinant protein remains a challenge probably due to the toxicity of *Apollo* overexpression in diverse biological systems, from prokaryotes to eukaryotes (personal communications).

Several genome-wide association studies previously highlighted correlations between *Apollo* SNP and different types of cancers [39–41]. In particular, the breast cancer-associated *Apollo* SNP rs11552449 (c.181C>T, p.His61Tyr) [40] was shown to increase the amount of Apollo transcripts including exon 2 and to result in higher ICLs and DSBs sensitivity in LLB cell lines generated from heterozygous carrier patients [41,49]. Until now, these were the only studies suggesting a causal association between *Apollo* and cancer. In our study, we demonstrated a significant telomere deprotection in *Apollo*$^{-/-}$ renal HKC8 cells expressing the *Apollo*^{N246I} and *Apollo*^{Y273H} mutants. To date, this type of *Apollo*-associated telomere phenotype has only been associated with HH syndrome arising very early in life [34,37]. Interestingly, patients with the telomere biology disorder dyskeratosis congenita are predisposed to develop cancers, especially head and neck squamous cell carcinoma (HNSCC) and leukemia [50,51]. In addition, a recent large-scale study demonstrated an association between cancer, mostly leukemia, and heterozygous germline mutations in telomerase and other telomere-maintenance genes [52]. As a shelterin complex-associated protein, Apollo may thus be considered as a new gene of interest in cancer predisposition. In fact, while high-degree Apollo dysfunctions are more likely to drive severe and early onset pathologies such as HH syndrome, one can imagine that in a heterozygous context, a more moderate phenotype could arise later in life due to the co-expression of the mutated and WT alleles. Thus, our current hypothesis is that RCC patients carrying heterozygous *Apollo*^{N246I} or *Apollo*^{Y273H} mutations combined with an *Apollo*^{WT} allele would be subjected to *Apollo* haploinsufficiency, leading to partial telomere fragility.

To conclude, we showed that the *Apollo*^{N246I} and *Apollo*^{Y273H} mutants identified in patients with ccRCC fail to protect telomere in the HKC8 human renal cell line. While further studying the activities of Apollo in different renal cell models is necessary, these results suggest that both Apollo mutants could participate in the onset of chromosome instability leading to oncogenesis in renal cells. Then, our study emphasizes the need to further explore the role of *Apollo* deficiency as a new putative driver of renal oncogenesis.

CRediT authorship contribution statement

Charlie Bories: Formal analysis, Investigation, Writing – original draft, Writing – review & editing. **Thomas Lejour:** Formal analysis, Investigation. **Florine Adolphe:** Formal analysis, Investigation, Writing – review & editing. **Laëtitia Kermasson:** Investigation, Methodology. **Laura Tanguy:** Investigation. **Gabriela Luszczewska:** Investigation. **Manon Watzky:** Investigation, Writing – review & editing. **Victoria Poillerat:** Investigation. **Pauline Garnier:** Investigation. **Regina Groisman:** Methodology, Writing – review & editing. **Sophie Ferlicot:** Formal analysis, Investigation. **Stéphane Richard:** Funding acquisition. **Murat Saparbaev:** Formal analysis, Writing – review & editing. **Patrick Revy:** Formal analysis, Writing – review & editing. **Sophie Gad:** Conceptualization, Formal analysis, Funding acquisition, Investigation, Writing – original draft, Writing – review & editing. **Flore Renaud:** Conceptualization, Funding acquisition, Investigation, Project administration, Supervision, Validation, Writing – original draft, Writing –

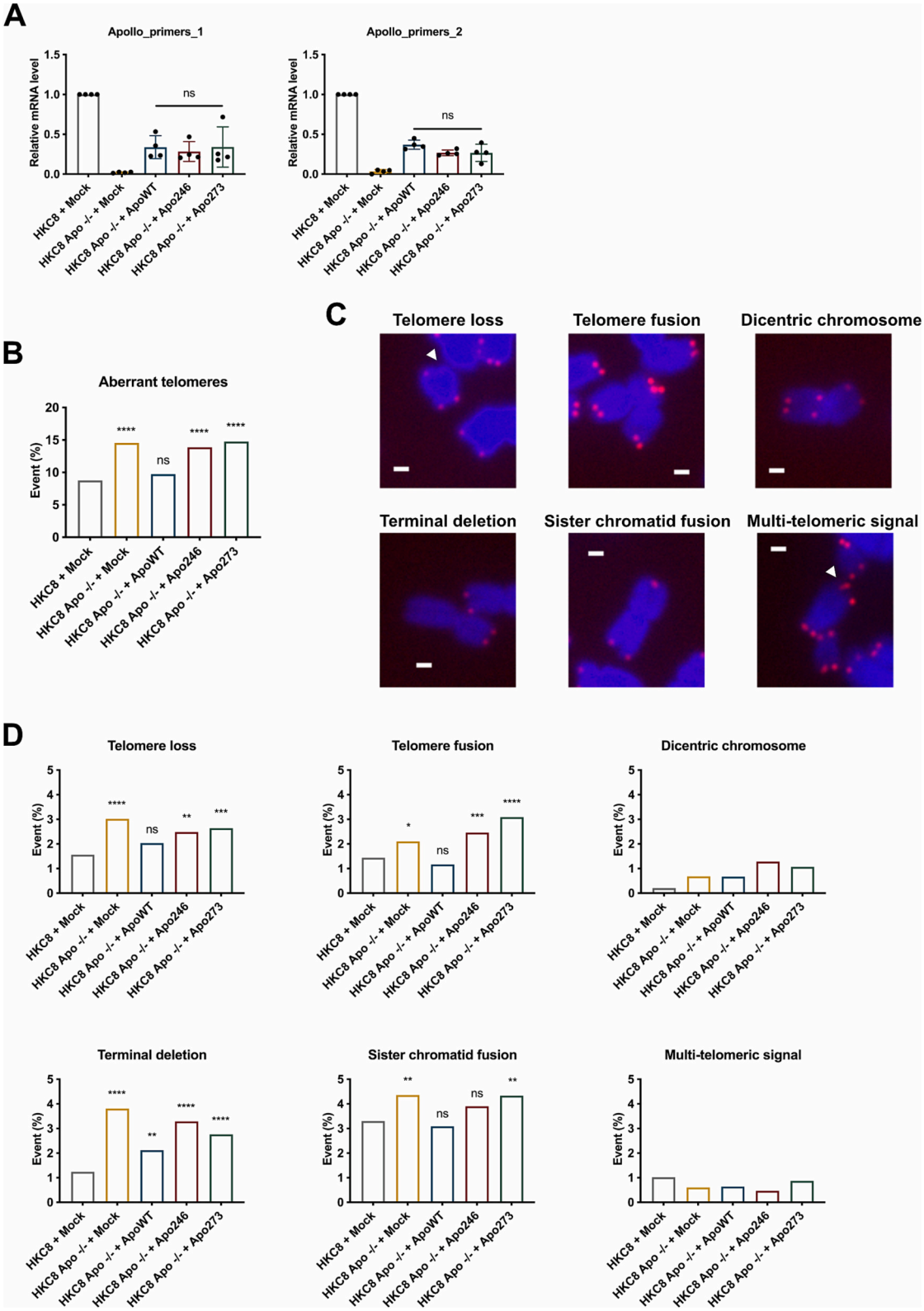

Fig. 6. Telomere aberrations associated with WT and mutants *Apollo* expression. A *Apollo* transcripts quantification relative to control genes *PPIA* and *HPRT1* in parental and *Apollo*$^{-/-}$ HKC8 stable cell lines expressing *Apollo*^{WT} (*ApoWT*), *Apollo*^{N246I} (*Apo246*), *Apollo*^{Y273H} (*Apo273*), or the control empty vector (Mock). Both primer pairs were used for RT-qPCR experiments. Mean and standard deviations from 4 independent stable transfection experiments are represented. Statistic derived from one-way ANOVA with $\alpha = 0.05$. ns: non-significant. **B** Quantification of global telomere aberrations detected by FISH in parental and *Apollo*$^{-/-}$ HKC8 stable cell lines expressing *Apollo*^{WT} (ApoWT), *Apollo*^{N246I} (Apo246), *Apollo*^{Y273H} (Apo273), or the control empty vector (Mock). Results represent the frequency of aberrations from 4 independent stable transfection experiments. Number of chromosomes analyzed: HKC8 + Mock: n = 4033; HKC8 *Apo*$^{-/-}$ + Mock: n = 3810; HKC8 *Apo*$^{-/-}$ + ApoWT: n = 3591; HKC8 *Apo*$^{-/-}$ + Apo246: n = 4229; HKC8 *Apo*$^{-/-}$ + Apo273: n = 3557. Statistics were derived from the chi-square test with HKC8 + Mock as reference and $\alpha = 0.05$. ns: non-significant, *: $p < 0.05$, **: $p < 0.01$, ***: $p < 0.001$, ****: $p < 0.0001$. **C** Representative pictures of telomere aberrations counted in B and D. Scale bar = 1 μM. **D** Detailed classification of telomere aberrations from B.

review & editing, Formal analysis.

Declaration of competing interest

The authors declare that they have no known competing financial interests or personal relationships that could have appeared to influence the work reported in this paper

Data availability

Data will be made available on request.

Acknowledgements

We thank the patients for their participation. We are grateful to "Centres de Ressources Biologiques" (CRB) from Necker and Cochin Hospitals for fixed tumors. We also thank Nathalie Droin for WES, Marc Deloger and Bastien Job for bioinformatic analyses, Brigitte Bressac for *in silico* analyses, the Taplin Biological Mass Spectrometry Facility (Harvard Medical School, Boston, USA) for running the mass spectrometry analysis, and the Imaging and Cytometry Core Facility (PFIC) (Unit AMMICa, Gustave Roussy) for the expertise and advice in using instruments. This work was supported by grants from: "Fondation ARC", "Ligue Contre le Cancer Comité du Val de Marne (94)", "Ligue Comité des Yvelines (78)", Ligue Comité de l'Indre (36), "Association pour la Recherche sur les Tumeurs du Rein" (A.R.Tu.R.), and "Taxe d'Apprentissage Gustave Roussy" (P25_MADU).

Appendix A. Supplementary data

Supplementary data to this article can be found online at https://doi.org/10.1016/j.bbadis.2024.167107.

References

[1] W.M. Linehan, et al., The metabolic basis of kidney cancer, Cancer Discov. 9 (8) (Aug. 2019) 1006–1021, https://doi.org/10.1158/2159-8290.CD-18-1354.
[2] J.J. Hsieh, et al., Renal cell carcinoma, Nat. Rev. Dis. Primer 3 (Mar. 2017), https://doi.org/10.1038/NRDP.2017.9.
[3] H. Hasumi, M. Yao, Hereditary kidney cancer syndromes: genetic disorders driven by alterations in metabolism and epigenome regulation, Cancer Sci. 109 (3) (Mar. 2018) 581–586, https://doi.org/10.1111/CAS.13503.
[4] F. Latif, et al., Identification of the von Hippel-Lindau disease tumor suppressor gene, Science 260 (5112) (1993) 1317–1320, https://doi.org/10.1126/SCIENCE.8493574.
[5] C.J. Creighton, et al., Comprehensive molecular characterization of clear cell renal cell carcinoma, Nature 499 (7456) (2013) 43–49, https://doi.org/10.1038/NATURE12222.
[6] T.K. Choueiri, W.G. Kaelin, Targeting the HIF2-VEGF axis in renal cell carcinoma, Nat. Med. 26 (10) (Oct. 2020) 1519–1530, https://doi.org/10.1038/S41591-020-1093-Z.
[7] W.M. Linehan, et al., Comprehensive molecular characterization of papillary renal-cell carcinoma, N. Engl. J. Med. 374 (2) (Jan. 2016) 135–145, https://doi.org/10.1056/NEJMOA1505917.
[8] C.F. Davis, et al., The somatic genomic landscape of chromophobe renal cell carcinoma, Cancer Cell 26 (3) (2014) 319–330, https://doi.org/10.1016/J.CCR.2014.07.014.
[9] P.R. Benusiglio, et al., A germline mutation in PBRM1 predisposes to renal cell carcinoma, J. Med. Genet. 52 (6) (2015) 426–430, https://doi.org/10.1136/JMEDGENET-2014-102912.
[10] T. Popova, et al., Germline BAP1 mutations predispose to renal cell carcinomas, Am. J. Hum. Genet. 92 (6) (Jun. 2013) 974–980, https://doi.org/10.1016/J.AJHG.2013.04.012.
[11] B. Shuch, et al., Germline PTEN mutation Cowden syndrome: an underappreciated form of hereditary kidney cancer, J. Urol. 190 (6) (2013) 1990–1998, https://doi.org/10.1016/J.JURO.2013.06.012.
[12] L. Schmidt, et al., Germline and somatic mutations in the tyrosine kinase domain of the MET proto-oncogene in papillary renal carcinomas, Nat. Genet. 16 (1) (1997) 68–73, https://doi.org/10.1038/NG0597-68.
[13] S. Turajlic, et al., Deterministic evolutionary trajectories influence primary tumor growth: TRACERx renal, Cell 173 (3) (Apr. 2018) 595–610.e11, https://doi.org/10.1016/J.CELL.2018.03.043.
[14] T.R. Hartman, et al., Prevalence of pathogenic variants in DNA damage response and repair genes in patients undergoing cancer risk assessment and reporting a personal history of early-onset renal cancer, Sci. Rep. 10 (1) (Dec. 2020), https://doi.org/10.1038/s41598-020-70449-5.
[15] J.C. Na, N. Nagaya, K.H. Rha, W.K. Han, I.Y. Kim, DNA damage response pathway alteration in locally advanced clear-cell renal-cell carcinoma is associated with a poor outcome, Clin. Genitourin. Cancer 17 (4) (2019) 299–305, https://doi.org/10.1016/j.clgc.2019.05.004.
[16] Y. Ged, et al., DNA damage repair pathway alterations in metastatic clear cell renal cell carcinoma and implications on systemic therapy, J. Immunother. Cancer 8 (1) (Jun. 2020) e000230, https://doi.org/10.1136/JITC-2019-000230.
[17] E. Guo, C. Wu, J. Ming, W. Zhang, L. Zhang, G. Hu, The clinical significance of DNA damage repair signatures in clear cell renal cell carcinoma, Front. Genet. 11 (Jan. 2021), https://doi.org/10.3389/FGENE.2020.593039.
[18] S.E. Scanlon, D.C. Hegan, P.L. Sulkowski, P.M. Glazer, Suppression of homology-dependent DNA double-strand break repair induces PARP inhibitor sensitivity in VHL-deficient human renal cell carcinoma, Oncotarget 9 (4) (2017) 4647–4660, https://doi.org/10.18632/ONCOTARGET.23470.
[19] J.P. Pletcher, et al., The emerging role of poly (ADP-ribose) polymerase inhibitors as effective therapeutic agents in renal cell carcinoma, Front. Oncol. 0 (Jul. 2021) 2559, https://doi.org/10.3389/FONC.2021.681441.
[20] R.M. Chabanon, et al., PBRM1 deficiency confers synthetic lethality to DNA repair inhibitors in cancer, Cancer Res. 81 (11) (Jun. 2021) 2888–2902, https://doi.org/10.1158/0008-5472.CAN-21-0628.
[21] M. Schmiester, I. Demuth, SNM1B/Apollo in the DNA damage response and telomere maintenance, Oncotarget 8 (29) (2017) 48398–48409, https://doi.org/10.18632/ONCOTARGET.16864.
[22] J.B. Bae, et al., Snm1B/Apollo mediates replication fork collapse and S Phase checkpoint activation in response to DNA interstrand cross-links, Oncogene 27 (37) (Aug. 2008) 5045–5056, https://doi.org/10.1038/ONC.2008.139.
[23] I. Demuth, M. Digweed, P. Concannon, Human SNM1B is required for normal cellular response to both DNA interstrand crosslink-inducing agents and ionizing radiation, Oncogene 23 (53) (Nov. 2004) 8611–8618, https://doi.org/10.1038/SJ.ONC.1207895.
[24] I. Demuth, et al., Endogenous hSNM1B/Apollo interacts with TRF2 and stimulates ATM in response to ionizing radiation, DNA Repair 7 (8) (Aug. 2008) 1192–1201, https://doi.org/10.1016/J.DNAREP.2008.03.020.
[25] J.M. Mason, J.A.M. Sekiguchi, Snm1B/Apollo functions in the Fanconi anemia pathway in response to DNA interstrand crosslinks, Hum. Mol. Genet. 20 (13) (Jul. 2011) 2549–2559, https://doi.org/10.1093/HMG/DDR153.
[26] J.M. Mason, et al., The SNM1B/APOLLO DNA nuclease functions in resolution of replication stress and maintenance of common fragile site stability, Hum. Mol. Genet. 22 (24) (Dec. 2013) 4901–4913, https://doi.org/10.1093/HMG/DDT340.
[27] M. van Overbeek, T. de Lange, Apollo, an Artemis-related nuclease, interacts with TRF2 and protects human telomeres in S phase, Curr. Biol. CB 16 (13) (Jul. 2006) 1295–1302, https://doi.org/10.1016/J.CUB.2006.05.022.
[28] B.D. Freibaum, C.M. Counter, hSnm1B is a novel telomere-associated protein, J. Biol. Chem. 281 (22) (Jun. 2006) 15033–15036, https://doi.org/10.1074/JBC.C600038200.
[29] B.D. Freibaum, C.M. Counter, The protein hSnm1B is stabilized when bound to the telomere-binding protein TRF2, J. Biol. Chem. 283 (35) (Aug. 2008) 23671–23676, https://doi.org/10.1074/JBC.M800388200.
[30] C. Lenain, S. Bauwens, S. Amiard, M. Brunori, M.J. Giraud-Panis, E. Gilson, The Apollo 5′ exonuclease functions together with TRF2 to protect telomeres from DNA repair, Curr. Biol. CB 16 (13) (Jul. 2006) 1303–1310, https://doi.org/10.1016/J.CUB.2006.05.021.
[31] T. de Lange, Shelterin-mediated telomere protection, Annu. Rev. Genet. 52 (Nov. 2018) 223–247, https://doi.org/10.1146/ANNUREV-GENET-032918-021921.
[32] P. Wu, M. van Overbeek, S. Rooney, T. de Lange, Apollo contributes to G overhang maintenance and protects leading-end telomeres, Mol. Cell 39 (4) (Aug. 2010) 606–617, https://doi.org/10.1016/j.molcel.2010.06.031.
[33] Y.C. Lam, et al., SNMIB/Apollo protects leading-strand telomeres against NHEJ-mediated repair, EMBO J. 29 (13) (Jul. 2010) 2230–2241, https://doi.org/10.1038/EMBOJ.2010.58.
[34] L. Kermasson, et al., Inherited human Apollo deficiency causes severe bone marrow failure and developmental defects, Blood 139 (16) (Apr. 2022) 2427–2440, https://doi.org/10.1182/blood.2021010791.
[35] P. Wu, H. Takai, T. De Lange, Telomeric 3′ overhangs derive from resection by Exo1 and Apollo and fill-in by POT1b-associated CST, Cell 150 (1) (Jul. 2012) 39–52, https://doi.org/10.1016/J.CELL.2012.05.026.
[36] S. Akhter, Y.C. Lam, S. Chang, R.J. Legerski, The telomeric protein SNM1B/Apollo is required for normal cell proliferation and embryonic development, Aging Cell 9 (6) (Dec. 2010) 1047–1056, https://doi.org/10.1111/J.1474-9726.2010.00631.X.
[37] F. Touzot, et al., Function of Apollo (SNM1B) at telomere highlighted by a splice variant identified in a patient with Hoyeraal-Hreidarsson syndrome, Proc. Natl. Acad. Sci. USA 107 (22) (Jun. 2010) 10097–10102, https://doi.org/10.1073/PNAS.0914918107.
[38] P. Revy, C. Kannengiesser, A.A. Bertuch, Genetics of human telomere biology disorders, Nat. Rev. Genet. 24 (2) (Feb. 2023) 86–108, https://doi.org/10.1038/S41576-022-00527-Z.
[39] X.S. Liang, et al., Genetic variants in DNA repair genes and the risk of cutaneous malignant melanoma in melanoma-prone families with/without CDKN2A mutations, Int. J. Cancer 130 (9) (May 2012) 2062–2066, https://doi.org/10.1002/IJC.26231.
[40] K. Michailidou, et al., Large-scale genotyping identifies 41 new loci associated with breast cancer risk, Nat. Genet. 45 (4) (Apr. 2013) 353–361, https://doi.org/10.1038/NG.2563.

[41] S. Herwest, et al., The hSNM1B/Apollo variant rs11552449 is associated with cellular sensitivity towards mitomycin C and ionizing radiation, DNA Repair 72 (Dec. 2018) 93–98, https://doi.org/10.1016/J.DNAREP.2018.09.004.
[42] R. Natrajan, et al., Delineation of a 1Mb breakpoint region at 1p13 in Wilms tumors by fine-tiling oligonucleotide array CGH, Genes Chromosom. Cancer 46 (6) (Jun. 2007) 607–615, https://doi.org/10.1002/GCC.20446.
[43] F. Adolphe, et al., Germline mutation in the NBR1 gene involved in autophagy detected in a family with renal tumors, Cancer Genet. 258–259 (Nov. 2021) 51–56, https://doi.org/10.1016/J.CANCERGEN.2021.07.003.
[44] L.C. Racusen, et al., Cell lines with extended in vitro growth potential from human renal proximal tubule: characterization, response to inducers, and comparison with established cell lines, J. Lab. Clin. Med. 129 (3) (1997) 318–329, https://doi.org/10.1016/S0022-2143(97)90180-3.
[45] I. Callebaut, D. Moshous, J.P. Mornon, J.P. De Villartay, Metallo-beta-lactamase fold within nucleic acids processing enzymes: the beta-CASP family, Nucleic Acids Res. 30 (16) (Aug. 2002) 3592–3601, https://doi.org/10.1093/NAR/GKF470.
[46] B. Salewsky, M. Schmiester, D. Schindler, M. Digweed, I. Demuth, The nuclease hSNM1B/Apollo is linked to the Fanconi anemia pathway via its interaction with FANCP/SLX4, Hum. Mol. Genet. 21 (22) (Nov. 2012) 4948–4956, https://doi.org/10.1093/HMG/DDS338.
[47] M. Ishiai, et al., DNA cross-link repair protein SNM1A interacts with PIAS1 in nuclear focus formation, Mol. Cell. Biol. 24 (24) (2004) 10733–10741, https://doi.org/10.1128/MCB.24.24.10733-10741.2004.
[48] H.T. Baddock, et al., A phosphate binding pocket is a key determinant of exo-versus endo-nucleolytic activity in the SNM1 nuclease family, Nucleic Acids Res. 49 (16) (Sep. 2021) 9294–9309, https://doi.org/10.1093/NAR/GKAB692.
[49] J.L. Caswell, et al., Multiple breast cancer risk variants are associated with differential transcript isoform expression in tumors, Hum. Mol. Genet. 24 (25) (Dec. 2015) 7421–7431, https://doi.org/10.1093/HMG/DDV432.
[50] B.P. Alter, N. Giri, S.A. Savage, P.S. Rosenberg, Cancer in the National Cancer Institute inherited bone marrow failure syndrome cohort after fifteen years of follow-up, Haematologica 103 (1) (Jan. 2018) 30–39, https://doi.org/10.3324/HAEMATOL.2017.178111.
[51] B.P. Alter, N. Giri, S.A. Savage, P.S. Rosenberg, Cancer in dyskeratosis congenita, Blood 113 (26) (2009) 6549–6557, https://doi.org/10.1182/BLOOD-2008-12-192880.
[52] K.E. Schratz, et al., Cancer spectrum and outcomes in the Mendelian short telomere syndromes, Blood 135 (22) (May 2020) 1946–1956, https://doi.org/10.1182/BLOOD.2019003264.